

A LoRa-Based Emotion Estimation Scheme for Smart Home Automated Actions Using ELMs

Christos Karras*, Aristeidis Karras*, Georgios Drakopoulos[†], Dimitrios Tsolis*, Phivos Mylonas[†], Spyros Sioutas*

*Decentralized Systems Computing Group, Computer Engineering and Informatics Department, University of Patras, Greece
{c.karras, akarras, sioutas}@ceid.upatras.gr, dtsolis@upatras.gr

[†]Humanistic and Social Informatics Laboratory, Department of Informatics, Ionian University, Greece
{c16drak, fmylonas}@ionio.gr

Abstract—Emotion detection is crucial in many IoT deployments from an operational perspective with examples ranging from digital health to smart cities. This is particularly true in smart homes where the interaction between the local IoT ecosystem and the inhabitants are continuous, pervasive, and nuanced. More specifically, emotion estimation from human speech attributes is an integral architectural component of such ecosystems. In this work, we survey the emerging LPWAN technologies and after selecting the most optimal for our use-case, we propose an emotion estimation scheme based on LoRa wireless technology for automated actions in smart home environments. In particular, a voice recognition module coupled with a transmitter are installed in a car. Then, depending on the estimation outcome, the smart home may undertake one or more preemptive actions according to its configuration as the car passenger approaches. The prototype LoRa system has been tested with the widely-used TESS dataset with encouraging results as expressed in the emotion confusion matrix obtained from an extreme learning machine with various kernels. The preceding paves the way for adaptive smart homes tailored to the needs of their inhabitants.

Index Terms—Adaptive Smart Homes, IoT, Emotion Detection, Human Speech, LoRa, LPWAN, Extreme Learning Machine

I. INTRODUCTION

Since its initial inception IoT technology has rapidly become an integral part of smart home ecosystems with a wide array of traditional household appliances such as television sets, refrigerators, and coffee machines being upgraded to support digital functions [1]. As smart homes gain popularity as well as commercial potential, innovative approaches and competing wireless protocols emerge to support these functions [2]. In this context major research effort is placed on the physical and emotional well-being of inhabitants and guests.

As the smart home industry landscape evolves because of new technologies, there is an imperative need to keep up with smart devices so as to create ecosystems that inhabitants can perform certain everyday actions with ease. To the best of the knowledge of the authors there are few contributions to the topic of either LoRa-based smart home ecosystems such as [3] and [4] or of the communication between a smart building and a car, whether autonomous or not, which however treat more general subjects like the nature of wireless coupling [5] or parking considerations [6] [7]. Nevertheless, there is a gap in the bibliography right at the spot of a LoRa smart home

ecosystem cooperating with a car for improving the smart home experience, which is the principal motivation behind this work as well as the differentiation points from existing methodologies.

The primary research objective of this paper is the development of a two part smart home cooperative ecosystem built on LoRa technology capable of estimating the affective polarity of a user and acting based on it as appropriate. For instance, in response to a negative emotion assessment dim lighting or relaxed music may be selected to placate the inhabitant. In order to accomplish this, a LoRa microphone installed in a car transmits voice packets, so that the rest of the system located smart home can act well in advance depending on the user emotional polarity. Said polarity is estimated by an extreme learning machine (ELM) with a number of kernels including the sigmoid and the Gaussian. As a biometric security measure, the system recognizes only one voice per use.

The remainder of this paper is structured as follows. Section II provides an overview of smart home IoT ecosystems, speech recognition technology, and emotion state estimation. In section III the basics of LoRa technology as well as the proposed LoRa architecture are explained. Section IV describes the proposed emotion estimation methodology and the available smart home actions. In section V the results obtained from the experiments are analyzed, while in section VI future research directions and recommendations for further work are given. Finally, technical acronyms are explained the first time they are encountered in text.

II. RELATED WORK

Smart homes are central to human well-being and to this end a number of technologies have been proposed [6] [8]. The infrastructure of a smart home is defined by how devices connect with one another, how and where sensor and appliance data is stored, how data is processed and trends derived, and how the inhabitants interact with the home and conversely [9]. As new technologies evolve, the differences from early IoT designs grow to the point that this is currently the era of smart home 2.0 [2] and agriculture 2.0 [10]. Privacy is among the pressing challenges smart homes are currently facing with reliability

and interoperability [3] being also points of concern. Possible privacy mechanisms range from physical layer encryption [11] to algorithmic schemes [12] and blockchains.

Affective state estimation has long been a focal point of interdisciplinary research [13]. In social network analysis public sentiment towards events are paramount to political campaigns and digital marketing [14] to name only a few. Such an estimation can in turn be the basis for recommending actions or achieving objectives such as maintaining user retention in cultural portals. Affective prediction typically rely on emotional models such as the emotion wheel [15] or alternatively on ontological clustering in conjunction with psychological attributes. ELMs perform emotion estimation from speech in numerous ways including deep attributes with segment-level probability distributions [16] or by identifying utterance-level emotions [17].

Biometric identification technologies are rapidly gaining traction in security and access control applications, with a biometric feature being defined as any physiological or behavioral trait which can identify uniquely, up to a reasonable error tolerance, any human [18]. These include face characteristics and facial expressions, fingerprints, hand geometry, iris recognition, gait, and speech [19] [20]. Typically these are driven to a machine learning (ML) system [21]. Any such system should meet the conditions of universality, distinctiveness, permanence, and collectability to perform satisfactorily [22].

III. LoRa ARCHITECTURE

A. LoRa ecosystem

LoRa is a recent innovation with the brand name established in the market in 2015¹. It runs on an unlicensed spectrum band below 1GHz with the actual central frequency being location-dependent in order to establish as the acronym itself suggests long-range communication links reaching up to 6Km [23]. It relies on a proprietary modified chirp spread spectrum modulation (CSS) that prioritizes sensitivity above throughput, especially for limited bandwidth [24]. This is ideal for smart homes where both power efficiency and security are required. A LoRa system consists of three major components as shown below [25]:

- **End-devices:** Devices such as sensors and actuators linked to one or more LoRa gateways through the LoRa radio interface.
- **Gateways:** Collective endpoints connecting end-devices with the LoRa NetServer, namely the network core element.
- **NetServer:** It manages the underlying network with tasks such as radio resources management, admission control, and security.

The received signal strength indication (RSSI) is the most common LoRa signal quality metric [13]. It refers to the received signal power in milliwatts and depends heavily on noise and on a number of indoor or outdoor factors including temperature, atmospheric electric charge and density, rainfall,

and humidity. Recent studies show a positive RSSI correlation with air temperature, on-board temperature, and solar radiation in outdoor environments during the day which vanishes during the night [26]. RSSI ranges from zero to -120 dBm, below which communication is impossible. Values down to -30 dBm denote a strong signal, while those between -30 dBm and -60 dBm a moderate one.

A generalization of RSSI is the signal to interference ratio (SIR) which besides noise considers distortions due to other wireless sources as well as delayed and distorted copies of the original signal. The latter come from the propagation properties of the immediate vicinity such as the geometry and the materials which may well lead to signal attenuation or multipath scattering. The above factors can severely degrade the performance of any wireless system. Typical LoRa SIR operating values range between -20 dB and $+10$ dB with higher values denoting more favorable signal propagation conditions.

LoRa equipment is designed to compensate for these adverse effects. Specifically at the physical layer the LoRa network depends on CSS in conjunction with an array of Gateways as part of the Gateway. The multichannel and multimodem Gateway array capacity allows the Netserver to receive a plurality of packets from the End-devices, effectively implementing a multiple input multiple output (MIMO) strategy. By assigning a unique spreading factor to each End-device, the mutual orthogonal signal separation is achieved.

The connections between the fundamental LoRa modulation parameters [27] are shown in table I. The CSS spread factor β_0 determines the number of orthogonal channels, whereas the code rate r_0 controls the redundancy inserted for error correction, trading off dynamically resilience with bandwidth. Eventually, per the LoRa datasheet one chip is delivered each second per Hz of bandwidth.

TABLE I
BASIC LoRa MODULATION PARAMETERS AND EQUATIONS.

Parameter	Meaning	Definition
L_0	Maximum LoRa range (km)	6
W_0	Modulation bandwidth (Hz)	See table II
θ_0	Car-home RSSI limit (dBm)	-80
β_0	Spreading factor	$7 - 12$
r_0	Code rate	$1 - 4$
R_b	Bit rate (bps)	$1/(2W_0)$
R_s	Symbol rate (symbols/sec)	$W_0/2^{\beta_0}$
R_c	Chip rate (chips/sec)	$4R_s/(4 + r_0)$

LoRa has a number of advantages compared to other wireless technologies such as SigFox and NB-IoT as shown in table II where key features are listed. Generally, LoRa tends to have good range and coverage, while at the same time is easier to be deployed than the other available technologies.

B. System architecture

The proposed system implementation consists of $1 \times$ Geetech Voice Recognition Module with Microphone for Arduino, $2 \times$

¹<https://loro-alliance.org/>

TABLE II
COMPARISON OF LPWAN TECHNOLOGIES (COMPILED FROM [28] [29] [30] [31] [32] [33] [34]).

Parameter	LoRa	SigFox	NB-IoT	LTE-M	DASH7
Standard	LoRa Alliance	SigFox / ETSI LTN	3 GPP Release 13,14	3 GPP	Dash Alliance
Bandwidth	250 kHz	100 Hz	200 kHz	1.4-20 MHz	433/868/915 MHz
Modulation	FSS/CSS	D-BPSK	QPSK	DL: OFDMA, 16 QAM	GFSK
Spectrum	1175 kHz	200 kHz	200 kHz	Licensed LTE bands	Licensed
Frequency band	EU : 868MHz	EU : 868MHz	7 – 900MHz	Cellular Band	Cellular Band
Transmission	FHSS (Aloha)	UNB	FDD	FDD/TDD	BLAST
Topology	Star-of-stars	Star	Star	Star	Half
Security	AES 128b	Optional encryption	NSA AES 256	AES 256	AES 128
Range (Urban)	2 – 5 km	3 – 10 km	1 – 5 km	1 – 5 km	1 km
Range (Rural)	20 km	50 km	10 – 15 km	10 – 15 km	2 km
Data Rate (Min)	250 <i>bps</i>	100 <i>bps</i>	100 <i>kbps</i>	1 <i>Mbps</i>	27.8 <i>kbps</i>
Data Rate (Max)	50 <i>kbps</i>	600 <i>bps</i>	200 <i>kbps</i>	4 <i>Mbps</i>	200 <i>Kbps</i>
Throughput	50 <i>kbps</i>	-	127 <i>Kbit</i>	1 <i>Mbit</i>	167 <i>kbit</i>
Energy Consumption	Very Low	Low	Medium Low	Medium	Low
Battery Life	~ 10 years	~ 12 years	~ 10 years	~ 2 years	~ 10 years
Deployment Cost	Moderate	Moderate	High	High	Moderate

LilyGO TTGO T-Beam v1.0 ESP32 LoRa 868 Mhz Arduino Board, 1× Raspberry Pi 4 Model B/4GB, 2× Sony Batteries IMR 18650 3000mAh, and Jumper wires for connectivity and signal transfer. Figure 1 depicts the architecture of the proposed system.

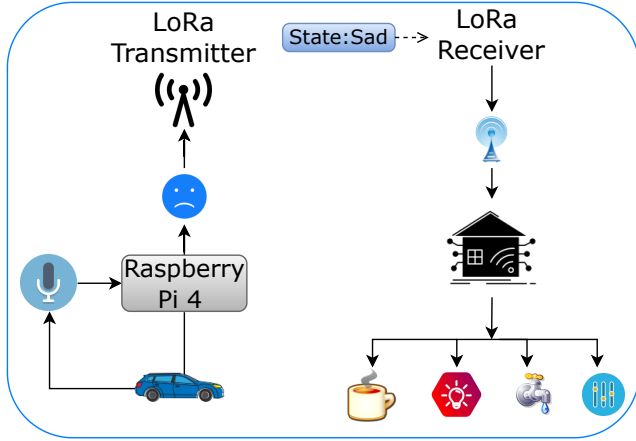


Fig. 1. System architecture.

As a consequence, the LoRa transmitter connects with the LoRa gateway when the RSSI between them exceeds θ_0 dBm, which in most cases results in satisfactory reception. After a successful connection, the Net-Server executes the proposed emotion estimation methodology and notifies the smart home ecosystem. As anticipated, certain devices are activated in response to certain emotional states, while others are deactivated. In order to make the proposed system more reliable and secure, it was trained to identify and respond to the speech emotional cues of only a single individual per use session.

The LoRa NetServer was installed on a Raspberry Pi 4 which is portable enough to qualify as part of the smart home

ecosystem IoT and also sufficiently powerful to run Python 3.9.0 with *numpy* and *scipy* and the *pip* package manager over Ubuntu. The latter are the platform for the proposed methodology.

IV. AFFECTIVE POLARITY ESTIMATION

A. Model

Estimating emotion polarity can be done in a number of ways. In the proposed approach an ELM estimates the emotion from speech and subsequently they determine polarity as shown in table VI. Since there is a plethora of emotion models with the most prominent ones listed in table III, the simplest but also most extensible one of [15] was selected to keep the ELM structure complexity at reasonable levels given the constrained resources of the IoT implementation.

TABLE III
EMOTION MODELS (INSPIRED BY [35]).

Model	Emotions	Approach
Ekman [36]	6	Categorical
Shaver et al. [37]	6	Categorical
Oatley et al. [38]	5	Categorical
Plutchik [15]	32	Wheel
Circumplex Russell [39]	28	Dimensional
OCC - Ortony et al. [40]	22	Dimensional
Lovheim [41]	8	Dimensional

The primary emotions according to the affective model [15] are the neutral state, fear, sadness, disgust, surprise, anger, and happiness. There is also provision for secondary and tertiary emotions as well as for non-linear composition operations for them. These comprise the Plutchik emotion wheel model.

B. ELM Training

ELMs rely on a single hidden layer of neurons and rely on the universal approximation theorem. As their output can be

analytically written in terms of the elements of the training vector and the activation function, they tend to learn faster in comparison to gradient-based neural network architectures as this explicit relationship lends itself to efficient training schemes, which are usually a linear least squares (LLS) problem. Moreover, there is no backward error magnification no need for derivative computations as there is only a single layer.

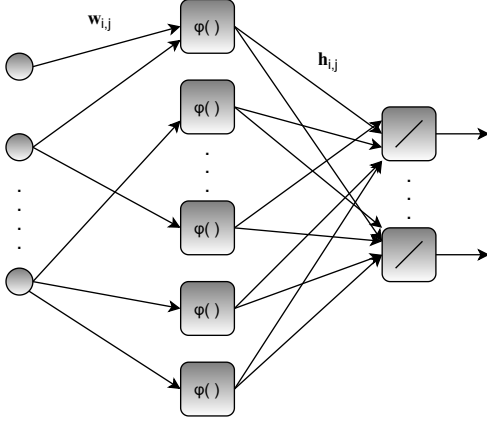


Fig. 2. ELM architecture.

The training dataset is the Toronto emotional speech set (TESS) collection [42] which is lightweight enough for the Netserver to handle and moreover it has exactly the same emotions with the reference model. The training attributes are energy, chroma, spectral entropy, spectral centroid, and cepstral coefficients.

In table IV the choices for the non-linearity $\varphi(\cdot)$ used in the experiments are shown. Observe that the kernels in the left column can take both positive and negative values while those in the right column only positive ones.

The weights $w_{i,j}$ connecting the attributes to the hidden layer are randomly chosen according to the Gaussian distribution (1). The latter is selected because of its six sigma property, namely that the overwhelming majority of its values lies in the interval $\mu \pm 3\sigma$. Also, the Gaussian distribution has the maximum differential entropy over all distributions of the same variance, meaning it explains more probabilistic scenarios than any other member of that class. Each such weight is selected independently from the input and neurons it connects.

$$f_W(w_{i,j}) \triangleq \frac{1}{\sigma\sqrt{2\pi}} \exp\left(-\frac{(w_{i,j} - \mu)^2}{2\sigma^2}\right) \quad (1)$$

On the contrary, the synaptic weights $h_{i,j}$ connecting the hidden layer to the output are variable and are in fact the part of the ELM which can be trained. To see how, consider first the training vector \mathbf{x}_k of (2):

$$\mathbf{x}_k \triangleq [x_{k,1}, x_{k,2}, \dots, x_{k,L_i}]^T \in \mathbb{R}^{L_i} \quad (2)$$

First the elements of \mathbf{x}_k are driven to the input layer ELM. Then, $x_{k,i}$ is driven to the j -th hidden neuron multiplied by

$w_{i,j}$ and added to the rest of the weighted elements such that the input $u_{k,j}$ would be as in (3):

$$u_{k,j} \triangleq \sum_{i=1}^{L_i} \mathbf{x}_{k,i} w_{i,j} = \mathbf{x}_k^T \mathbf{w}_j \quad (3)$$

The intermediate inputs u_j are driven to the respective hidden neurons in order to generate the output $\varphi(u_j)$. Considering all training vectors for every hidden neuron results in the matrix \mathbf{A} of equation (4) where p and L_h denote the number of training vectors and the hidden layer size respectively.

$$\mathbf{A} \triangleq \begin{bmatrix} \varphi(u_{1,1}) & \varphi(u_{1,2}) & \dots & \varphi(u_{1,L_h}) \\ \vdots & \vdots & \ddots & \vdots \\ \varphi(u_{p,1}) & \varphi(u_{p,2}) & \dots & \varphi(u_{p,L_h}) \end{bmatrix} \in \mathbb{R}^{p \times L_h} \quad (4)$$

Determining the $L_h L_u$ weights $h_{i,j}$ is reduced to an LLS problem with respect to matrix \mathbf{H} where the latter contains them stacked as in equation (5):

$$\mathbf{H} \triangleq \begin{bmatrix} h_{1,1} & h_{2,1} & \dots & h_{L_h,1} \\ h_{1,2} & h_{2,2} & \dots & h_{L_h,2} \\ \vdots & \vdots & \ddots & \vdots \\ h_{1,L_u} & h_{2,L_u} & \dots & h_{L_h,L_u} \end{bmatrix} \quad (5)$$

This matrix can be computed as the solution of the LLS of (6):

$$\hat{\mathbf{H}} \triangleq \min \{\|\mathbf{A}\mathbf{H} - \mathbf{T}\|_2\} \quad (6)$$

The solution can be obtained as in (7) but it is rarely if ever computed this way. Instead, other methods are preferable such as the QR factorization, incomplete Cholesky, or regularized methodologies such as the one of (8).

$$\hat{\mathbf{H}} = (\mathbf{A}^T \mathbf{A})^{-1} \mathbf{A}^T \mathbf{T} \quad (7)$$

The regularized form of (7) is (8) and relies on the insertion of an additional factor in order to improve the numerical condition of the coefficient matrix at the expense of solution accuracy. Still, since LLS is a statistical approximation, small values of the regularization hyperparameter ρ_0 have little effect.

$$\hat{\mathbf{H}} = (\mathbf{A}^T \mathbf{A} + \rho_0 \mathbf{I})^{-1} \mathbf{A}^T \mathbf{T} \quad (8)$$

For our experiments the regularization hyperparameter ρ_0 was set equal to the minimum non-zero eigenvalue of the coefficient matrix.

An iterative scheme for solving the LLS as well as its regularized version is the conjugate gradient. It can be executed only when the coefficient matrix is symmetric and positive definite, but in practice it may work for positive semidefinite matrices as well. It is a matrix-free method as it relies on the effect a given matrix has on a vector rather than on the structure of the matrix itself.

The parameters of the ELM training are listed in table V.

C. Smart home actions

The ability of smart homes to act is second in importance only to their capacity to sense. In table VI are listed possible

TABLE IV
ELM HIDDEN LAYER ACTIVATION FUNCTIONS.

Function	Formula	Function	Formula
Hyperbolic tangent	$\gamma_1 \tanh(\gamma_0 u)$	Sigmoid	$\frac{1}{1 + \exp(-\gamma_0 u)}$
Inverse linear	$\frac{\gamma_1}{1 + \gamma_0 u}$	Inverse square	$\frac{\gamma_1}{1 + \gamma_0 u^2}$

TABLE V
ELM TRAINING PARAMETERS.

Parameter	Meaning	Value
μ	Synaptic weight mean	0
σ^2	Synaptic weight variance	1
L_i	Length of input layer	23
L_h	Length of hidden layer	47
L_u	Length of output layer	7
train/test/validation	Train/test/validation (%)	70/20/10

actions a typical smart home can perform, namely controlling the temperature, music, lighting, preparing warm water for shower, and operating a smart coffee machine. In the proposed approach the actions depend only on the emotional polarity. As surprise is pleasant in the TESS collection, it is classified as having positive polarity.

TABLE VI
ACTIONS VS. EMOTIONAL POLARITY (FROM [1] [3] [6] AND REFERENCES THEREIN).

Polarity	Emotions	Actions	Feedback (P/N%)
Neutral	Neutral	Dim lighting	86.38/10.15
		Pleasant music	83.19/11.37
		Mild temperature	81.45/12.45
		Warm water	79.21/11.75
Positive	Happiness	Bright lighting	77.25/14.33
	Surprise	Upbeat music	76.12/15.88
		Coffee	75.88/16.92
Negative	Disgust	Soothing music	73.68/18.67
	Fear	Normal lighting	72.57/19.28
	Anger	Warm water	69.15/21.92
	Sadness	Coffee	67.38/24.12

The actions listed in table VI are indicative and have been extracted from the relevant scientific literature. The reasons for selecting them are the following:

- They cover all five senses, giving an integrated experience to the inhabitants.
- They are among the less intrusive actions compared to others available.
- They appear frequently in studies reflecting a strong preference to them.
- Their total feedback in these studies is positive.

The feedback in the rightmost column of table VI comes from the literature survey coming from the main references

of this table as well as from their respective references. With specific positive and negative mentions counting as one positive or negative point respectively while no reference at all amounts to a neutral point. The listed actions are ranked based on the ratio of their positive points to the total of positive, negative, and neutral ones.

The requirement for action subtlety comes from the robotics *uncanny valley* principle which in the context of smart homes can be translated as that the latter cannot act *too* human. A solution would be that actions are merely affective hints. On the contrary, a constant emotional nudging is likely to be perceived as invasive, especially when the inhabitants are negatively emotionally charged.

V. RESULTS

A. Emotion estimation heatmap

The heatmap of figure 3 strongly hints that ELM, properly trained and at least under moderately favorable circumstances in urban settings, can separate the basic emotions of the TESS reference dataset very well. This can be confirmed from the metrics of table VII, which are standard for evaluating classification tasks.



Fig. 3. Emotion heatmap (Best kernel, optimal SIR).

TABLE VII
CONFUSION MATRIX METRICS (BEST KERNEL, OPTIMAL SIR).

Metric	Score	Metric	Score
Precision	0.8617	phi coefficient	0.5908
Recall	0.8585	Markedness	0.6912
Accuracy	0.8587	False positive rate	0.0393
F1	0.8601	False negative rate	0.0511

Consistent with findings from earlier research such as for instance [43] and [44] no emotion is perfectly recognized

even under the best possible conditions as revealed from the emotion heatmap. The neutral state is occasionally mistaken as disgust, sadness, or fear. Sadness can be explained by its low valence and subtlety, fear may lead to caution which can be interpreted as a neutral stance, and disgust has a subtext of intentional distance from a person, object, or situation [45]. Another common mistake is between happiness and surprise since they both can be strong feelings. The emotion which is hardest to discover is disgust, as it appears to have relatively strong components of fear and surprise [46].

B. Kernel Selection

In table VIII the residual mean square error (RMSE) and the number of iterations are listed for each ELM configuration, namely kernel and regularization pair.

TABLE VIII
ELM TRAINING EFFICIENCY VS KERNELS (BEST SIR).

ELM	RMSE	Iters.
HT	0.0031	42
S	0.0076	61
IL	0.0083	78
IS	0.0114	83
HT+R	0.0037	46
S+R	0.0051	55
IL+R	0.0063	67
IS+R	0.0099	71

The difference in the kernel performance can be attributed to the fact that the hyperbolic tangent (HT) kernel is smooth enough, bounded, and with enough variability to piecewise approximate most target functions. The sigmoid (S) kernel lacks the latter as it is confined to positive values only. The inverse linear (IL) kernel on the other hand can take negative values but it is rather inflexible compared to the previous kernels. When the synaptic weights $w_{i,j}$ are non-negative, then the sigmoid kernel is frequently the clear winner over the inverse linear. However, when $w_{i,j}$ can also be negative, then their difference in performance may well be a close call depending on the actual numerical values of the weights. Finally, the inverse square (IS) kernel is neither flexible nor expanding to the entire range of $w_{i,j}$ and thus it yields high errors. Therefore, its use is recommended only in special cases where its particular form is a good fit.

Regularization appears to remedy up to an extent the problems of the lower performing kernels. This may be explained from the fact that the latter generate an defective eigenspace with a dimensionality much lower than that of the original coefficient matrix, perhaps because the kernel itself does not generate intermediate outputs with sufficient variability. The addition of the regularizing term corrects this by supplying enough orthogonal eigenvectors which leads to a solution – albeit a distorted one. The regularization effect is also reflected to the reduced number of iterations as the improved numerical condition of the coefficient matrix leads to a quicker solution.

C. The Effect Of SIR

Here the performance of the ELM is evaluated with respect to the SIR. The latter was deliberately chosen over RSSI as wireless devices rarely operate isolated in an urban environment. The SIR range represents reported urban conditions [27], with optimal SIR being the same with the previous subsection. Although the SIR per se is not an attribute extracted from the voice segments of the TESS dataset, it influences their values since a severely degraded signal is bound to contain corrupted attributes. The values reported in table IX are for the best ELM training configuration, namely the hyperbolic tangent kernel, and it can be observed that low SIR values can degrade ELM performance. Therefore, it is recommended that in a wireless setting, techniques for ensuring signal quality should be put in place, since the latter can be the subject of further processing.

TABLE IX
HT KERNEL RMSE VS. SIR

HT	10m	100m
30 dB	0.0031	0.0033
20 dB	0.0031	0.0036
15 dB	0.0037	0.0044
10 dB	0.0038	0.0049
5 dB	0.0041	0.0057
0 dB	0.0053	0.0062

VI. CONCLUSIONS AND FUTURE WORK

Smart homes are the epicenter of intense interdisciplinary research as they are paramount to human well-being. This paper focuses on a two-part smart home ecosystem built on the emerging LoRa wireless technology. The first half is installed in a car, which need not be autonomous, and transmits attributes extracted from speech to the second half, located at the smart home, which estimates the emotional state of the driver with an extreme learning machine. Then, the smart home undertakes subtle actions, inspired by the uncanny valley robotics principle, depending on the estimated affective polarity. This approach differs from existing ones in that no LoRa smart home ecosystems, to the best of the knowledge of the authors, perform emotion estimation. Moreover, although cases of smart buildings cooperating with cars have been presented, very few do so for smart home purposes. The results indicate a superb performance of the emotion estimation and consistency with reported misclassification.

This paper can be extended in a number of ways. First and foremost, experiments with more datasets can be conducted in order to better understand why and how emotion misclassification happens. Moreover, more prediction models can be added perhaps requiring more attributes so that a stacking or bagging methodology can be applied to their combined outcomes. In particular, this can be used to obtain higher granularity emotion estimation which will enable the smart home to undertake actions tailored to each of the seven basic emotional states mentioned in this work.

REFERENCES

- [1] D. B. Gannon, D. A. Reed, and J. R. Larus, "Imagining the future: Thoughts on computing," *Computer*, vol. 45, no. 01, pp. 25–30, 2012.
- [2] M. Chen, J. Yang, X. Zhu, X. Wang, M. Liu, and J. Song, "Smart Home 2.0: Innovative smart home system powered by botanical IoT and emotion detection," *Mobile Networks and Applications*, vol. 22, pp. 1159–1169, 2017.
- [3] E. Gambi, L. Montanini, D. Pigni, G. Ciattaglia, and S. Spinsante, "A home automation architecture based on LoRa technology and message queue telemetry transfer protocol," *International Journal of Distributed Sensor Networks*, vol. 14, no. 10, 2018.
- [4] R. Islam, M. W. Rahman, R. Rubaiat, M. M. Hasan, M. M. Reza, and M. M. Rahman, "LoRa and server-based home automation using the internet of things (IoT)," *Journal of King Saud University – Computer and Information Sciences*, 2021.
- [5] H. Ullah, N. Gopalakrishnan Nair, A. Moore, C. Nugent, P. Muschamp, and M. Cuevas, "5G Communication: An overview of vehicle-to-everything, drones, and healthcare use-cases," *IEEE Access*, vol. 7, no. 1, pp. 37251–37268, 2019.
- [6] F. Al-Turjman and A. Malekloo, "Smart parking in IoT-enabled cities: A survey," *Sustainable Cities and Society*, vol. 49, 2019.
- [7] A.-M. Kamyli, S. Kontogiannis, D. Kyriadiis, and C. Zaroliagis, "Incentivizing Truthfulness in Crowdsourced Parking Ecosystems," in *2021 IEEE International Smart Cities Conference (ISC2)*, pp. 1–7, IEEE, 2021.
- [8] Dragos Mocrii, Yuxiang Chen, and Petr Musilek, "IoT-based smart homes: A review of system architecture, software, communications, privacy and security," *Internet of Things*, vol. 1-2, pp. 81–98, 2018.
- [9] P. A. Alaba, S. I. Popoola, L. Olatomiwa, M. B. Akanle, O. S. Ohunakin, E. Adetiba, O. D. Alex, A. A. Atayero, and W. M. A. Wan Daud, "Towards a more efficient and cost-sensitive extreme learning machine: A state-of-the-art review of recent trend," *Neurocomputing*, vol. 350, pp. 70–90, 2019.
- [10] A. Karras, C. Karras, G. Drakopoulos, D. Tsois, P. Mylonas, and S. Sioutas, "SAF: A Peer to Peer IoT LoRa System for Smart Supply Chain in Agriculture," in *IFIP International Conference on Artificial Intelligence Applications and Innovations*, pp. 41–50, Springer, 2022.
- [11] J. Zhang, T. Q. Duong, R. Woods, and A. Marshall, "Securing Wireless Communications of the Internet of Things from the Physical Layer, An Overview," *Entropy*, vol. 19, no. 8, 2017.
- [12] Gang Sun, Victor Chang, Muthu Ramachandran, Zhili Sun, Gangmin Li, Hongfang Yu, and Dan Liao, "Efficient location privacy algorithm for Internet of Things (IoT) services and applications," *Journal of Network and Computer Applications*, vol. 89, pp. 3–13, 2017. Emerging Services for Internet of Things (IoT).
- [13] M. Anjum, M. A. Khan, S. Ali Hassan, A. Mahmood, and M. Gidlund, "Analysis of RSSI fingerprinting in LoRa networks," in *IWCMC*, pp. 1178–1183, 2019.
- [14] D. Al Hajjar and A. Z. Syed, "Applying sentiment and emotion analysis on brand tweets for digital marketing," in *2015 IEEE Jordan Conference on Applied Electrical Engineering and Computing Technologies (AEECT)*, pp. 1–6, 2015.
- [15] R. Plutchick, "A general psychoevolutionary theory of emotion," in *Theories of Emotion* (R. Plutchik and H. Kellerman, eds.), pp. 3–33, Academic Press, 1980.
- [16] L. Guo, L. Wang, J. Dang, L. Zhang, and H. Guan, "A feature fusion method based on extreme learning machine for speech emotion recognition," in *ICASSP*, pp. 2666–2670, IEEE, 2018.
- [17] K. Han, D. Yu, and I. Tashev, "Speech Emotion Recognition Using Deep Neural Network and Extreme Learning Machine," in *Interspeech 2014*, September 2014.
- [18] A. Jain, A. Ross, and S. Prabhakar, "An introduction to biometric recognition," *IEEE Transactions on Circuits and Systems for Video Technology*, vol. 14, no. 1, pp. 4–20, 2004.
- [19] S. Z. Li and A. K. Jain, *Handbook of Face Recognition*. Springer, 2011.
- [20] D. Maltoni, *Handbook of Fingerprint Recognition*. Springer, 2009.
- [21] J. J. Winston and D. J. Hemanth, "A comprehensive review on iris image-based biometric system," *Soft Computing*, vol. 23, no. 19, pp. 9361–9384, 2019.
- [22] Shaymaa Adnan Abdulrahman and Bilal Alhayani, "A comprehensive survey on the biometric systems based on physiological and behavioural characteristics," *Materials Today: Proceedings*, 2021.
- [23] B. Islam, M. T. Islam, J. Kaur, and S. Nirjon, "LoRaIn: Making a case for LoRa in indoor localization," in *PerCom Workshops*, pp. 423–426, 2019.
- [24] R. S. Sinha, Y. Wei, and S.-H. Hwang, "A survey on LPWAN technology: LoRa and NB-IoT," *ICT Express*, vol. 3, no. 1, pp. 14–21, 2017.
- [25] L. Vangelista, A. Zanella, and M. Zorzi, "Long-range IoT technologies: The dawn of LoRa™," in *Future Access Enablers for Ubiquitous and Intelligent Infrastructures* (V. Atanasovski and A. Leon-Garcia, eds.), pp. 51–58, Springer International Publishing, 2015.
- [26] O. Elijah, S. K. A. Rahim, V. Sittakul, A. M. Al-Samman, M. Cheffena, J. B. Din, and A. R. Tharek, "Effect of weather condition on LoRa IoT communication technology in a tropical region: Malaysia," *IEEE Access*, vol. 9, 2021.
- [27] SEMTECH, "AN1200.22 LoRa™ modulation basics," 2015.
- [28] M. Singh Bali, K. Gupta, K. Kour Bali, and P. K. Singh, "Towards energy efficient NB-IoT: A survey on evaluating its suitability for smart applications," *Materials Today: Proceedings*, vol. 49, pp. 3227–3234, 2022.
- [29] M. I. Hossain and J. I. Markendahl, "Comparison of LPWAN Technologies: Cost Structure and Scalability," *Wireless Personal Communications*, vol. 121, no. 1, pp. 887–903, 2021.
- [30] J. Qin, Z. Li, R. Wang, L. Li, Z. Yu, X. He, and Y. Liu, "Industrial Internet of Learning (IIoL): IIoT based pervasive knowledge network for LPWAN—concept, framework and case studies," *CCF Transactions on Pervasive Computing and Interaction*, vol. 3, no. 1, pp. 25–39, 2021.
- [31] A. Khalifeh, K. A. Aldahdouh, K. A. Darabkh, and W. Al-Sit, "A Survey of 5G Emerging Wireless Technologies Featuring LoRaWAN, Sigfox, NB-IoT and LTE-M," in *2019 International Conference on Wireless Communications Signal Processing and Networking (WiSPNET)*, pp. 561–566, 2019.
- [32] W. Ayoub, A. E. Samhat, F. Nouvel, M. Mroue, and J.-C. Prévotet, "Internet of mobile things: Overview of lorawan, dash7, and nb-iot in lpwans standards and supported mobility," *IEEE Communications Surveys & Tutorials*, vol. 21, no. 2, pp. 1561–1581, 2018.
- [33] L. Oliveira, J. J. Rodrigues, S. A. Kozlov, R. A. Rabêlo, and V. H. C. d. Albuquerque, "Mac layer protocols for internet of things: A survey," *Future Internet*, vol. 11, no. 1, p. 16, 2019.
- [34] B. Shilpa, R. Radha, and P. Movva, "Comparative Analysis of Wireless Communication Technologies for IoT Applications," in *Artificial Intelligence and Technologies*, pp. 383–394, Springer, 2022.
- [35] K. Sailunaz, M. Dhaliwal, J. Rokne, and R. Alhaji, "Emotion detection from text and speech: A survey," *SNAM*, vol. 8, no. 1, pp. 1–26, 2018.
- [36] P. Ekman, "An argument for basic emotions," *Cognition and Emotion*, vol. 6, no. 3-4, pp. 169–200, 1992.
- [37] P. R. Shaver, J. C. Schwartz, D. Kirson, and C. O'Connor, "Emotion knowledge: Further exploration of a prototype approach," *Journal of personality and social psychology*, vol. 52, no. 6, pp. 1061–86, 1987.
- [38] K. Oatley and P. N. Johnson-laird, "Towards a cognitive theory of emotions," *Cognition and Emotion*, vol. 1, no. 1, pp. 29–50, 1987.
- [39] J. Russell, "A circumplex model of affect," *Journal of Personality and Social Psychology*, vol. 39, no. 12, pp. 1161–1178, 1980.
- [40] A. Ortony, G. L. Clore, and A. Collins, *The Cognitive Structure of Emotions*. Cambridge University Press, 1990.
- [41] H. Lövhheim, "A new three-dimensional model for emotions and monoamine neurotransmitters," *Medical Hypotheses*, vol. 78, no. 2, pp. 341–348, 2012.
- [42] K. Dupuis and M. K. M. Kathleen Pichora-Fuller, "Toronto emotional speech set (TESS)," 2010.
- [43] R. A. Khalil, E. Jones, M. I. Babar, T. Jan, M. H. Zafar, and T. Alhussain, "Speech emotion recognition using deep learning techniques: A review," *IEEE Access*, vol. 7, pp. 117327–117345, 2019.
- [44] Z.-T. Liu, M. Wu, W.-H. Cao, J.-W. Mao, J.-P. Xu, and G.-Z. Tan, "Speech emotion recognition based on feature selection and extreme learning machine decision tree," *Neurocomputing*, vol. 273, pp. 271–280, 2018.
- [45] A. Mehrabian, "Comparison of the pad and panas as models for describing emotions and for differentiating anxiety from depression," *Journal of Psychopathology and Behavioral Assessment*, vol. 19, no. 4, p. 331–357, 1997.
- [46] L. Shu, J. Xie, M. Yang, Z. Li, Z. Li, D. Liao, X. Xu, and X. Yang, "A Review of Emotion Recognition Using Physiological Signals," *Sensors*, vol. 18, no. 7, 2018.